Materials and Methods

Kinetic Models

Ligand binding is dependent on the amount of available receptors (B_{avail}) and the affinity of the ligand for the receptor ($1/K_D$). Practically, parameters that are related to this product (binding potential) can be determined in various ways (*1*). One substitute is the total distribution volume (V_T), which is the concentration of the radioligand in the brain region related to the concentration of the radioligand in plasma at equilibrium. The equilibrium V_T is composed of a specific distribution volume (V_S, equal to $f_P B_{avail}/K_D$, with f_P being the fraction of free ligand in plasma) and the distribution volume of free and nonspecifically bound ligand (V_{ND}). V_T was determined by the following models: the standard 1- and 2-tissue-compartment models with a blood volume fraction fixed at 0.03 mL/cm^3 (*2*) as implemented in PMOD (which was used for all subsequent models) (1TCM and 2TCM), and by Logan graphical analysis (GA) with a time of linearization t* = 40 min (*3*) and the multilinear graphical analysis MA1: this model is based on the GA approach but the expression is formulated as a multilinear equation with t* = 40 min (*4*). For GA and MA1 tissue, TACs were manually corrected for blood volume fraction according to $C_{PET} = 0.97 \times C_{Tissue} - 0.03 \times C_{WB}$.

The catheter used for blood sampling caused a time delay in the arterial input function. This delay was estimated with the "fit blood" option as implemented in PMOD and fixed for the further steps. It was on average 5.0 ± 3.8 s (n = 15).

For the bolus-plus-constant-infusion experiments, V_T was determined by the tissue-to-plasma ratio (TPR) during the steady-state phase (50–70 min). For TPR, the tissue activity (time–activity curve) was corrected manually for blood volume fraction as described above for GA and MA1. For kinetic analyses, only data up to 70 min were used (to allow inclusion of DPCPX competition studies).

Regional binding potentials related to the nondisplaceable uptake (BP_{ND}) as a second measure of ligand binding (*1*) was determined by the following kinetic models based on the olfactory bulb TAC as input:

- The simplified reference tissue model (SRTM) (*5*), which fits 3 parameters by nonlinear regression analysis: BP_{ND}; k_2', the efflux rate of the reference region; and R_1, a relative blood flow–associated parameter that is a ratio of the influx constants of target and reference region.

- The 2-step simplified SRTM version (SRTM2) (*6*): in theory k_2' is identical for all brain regions, which allows further simplification of the SRTM by fixing k_2' for all regions and thus reducing the number of fitted parameters.
- Logan noninvasive graphical analysis (NIGA) (*7*): the compartmental model equations can be rearranged in a linear equation allowing determination of $BP_{ND} + 1$ for reversibly binding ligands by calculating the slope of the linear regression. A prerequisite is again the previous determination of k_2'.
- The multilinear reference tissue model (MRTM) (*8*): this linearized reference tissue model is a further rearrangement of the NIGA approach by formulating multilinear equations. Three linear regression parameters are fitted to calculate BP_{ND}, R_1, and k_2'.
- The ratio of distribution volumes (DVR-1) from the V_T of the 2TCM in target and reference region (*9*).

The time point after which the transformed parameters of the graphical analysis became linear (t*) was selected on the basis of visual inspection of the residual plot. For NIGA, t* was set to 40 min. Predetermination of k_2' was done by averaging the parameters from low-noise regions from the SRTM (*8*). For MRTM, t* was set to 40 min.

Parametric images were generated representing BP_{ND} by the SRTM2 model on the voxel level with a predetermined k_2' of the average of low-noise regions from the SRTM (*6*). SRTM2 was determined with the basis function approach as implemented in PMOD 3.3. The parameter boundaries for k2a were 0.06 to 0.6 and the number of functions 400. For the reference tissue input models, time–activity curves were not corrected for blood volume fraction.

The goodness of fits was assessed with the Akaike information criteria, which included a penalty for increasing numbers of parameters in the model.

Autoradiography

Rats (n = 9) were decapitated, and their brains rapidly removed, frozen in 2-methylbutane (–40°C), and stored at −80°C. Ten brain sections per rat (20-μm thickness) were thaw-mounted onto sialin-coated slides (Starfrost adhesive; Knittel GmbH) and stored at −80°C. Preincubation in 200 mL of Tris-HCl buffer (170 mM; pH 7.4) for 15 min at 4°C was followed by 2 h of incubation at room temperature (RT) in 20 mL of buffer containing different concentrations of ^{3}H-DPCPX (0.125–8 nM; specific activity, 4,400 GBq/mmol), 2

units/mL adenosine deaminase, and 100 μM Gpp(NH)p. Nonspecific binding was determined by adding R-phenyl-iso-propyl-adenosine (100 μM) to the incubation buffer. After 2 washing steps in 200 mL of preincubation buffer (5 min, 4°C) and a rapid rinse in 200 mL of ice-cold water (15 s), the sections were dried in a stream of air (RT). Slides were exposed to phosphor-imaging plates (BAS2025; Fuji) together with industrial tritium activity standards (Amersham Biosciences) for 3 d. The stored information was retrieved with an image plate reader (spatial resolution, 50 μm; BAS 5000), and digital autoradiograms were further processed with dedicated image analysis software (Image Gauge 4.0; Fuji). Regions of interest (ROIs) were defined according to a standard rat brain atlas (*10*) and adapted to the ROIs used for PET. Nonspecific binding was determined for each concentration by linear fitting of the measured nonspecific values. Specific binding was then calculated as the difference between total and nonspecific binding.

References

(1) Innis RB, Cunningham VJ, Delforge J, et al. Consensus nomenclature for in vivo imaging of reversibly binding radioligands. *J Cereb Blood Flow Metab*. 2007;27:1533–1539.

(2) Adam JF, Elleaume H, Le Duc G, et al. Absolute cerebral blood volume and blood flow measurements based on synchrotron radiation quantitative computed tomography. *J Cereb Blood Flow Metab*. 2003;23:499–512.

(3) Logan J, Fowler JS, Volkow ND, et al. Graphical analysis of reversible radioligand binding from time-activity measurements applied to [N-^{11}C-methyl]-(–)-cocaine PET studies in human subjects. *J Cereb Blood Flow Metab*. 1990;10:740–747.

(4) Ichise M, Toyama H, Innis RB, Carson RE. Strategies to improve neuroreceptor parameter estimation by linear regression analysis. *J Cereb Blood Flow Metab*. 2002;22:1271–1281.

(5) Lammertsma AA, Hume SP. Simplified reference tissue model for PET receptor studies. *Neuroimage*. 1996;4:153–158.

(6) Wu Y, Carson RE. Noise reduction in the simplified reference tissue model for neuroreceptor functional imaging. *J Cereb Blood Flow Metab*. 2002;22:1440–1452.

(7) Logan J, Fowler JS, Volkow ND, Wang GJ, Ding YS, Alexoff DL. Distribution volume ratios without blood sampling from graphical analysis of PET data. *J Cereb Blood Flow Metab*. 1996;16:834–840.

(8) Ichise M, Liow JS, Lu JQ, et al. Linearized reference tissue parametric imaging methods: application to [^{11}C]DASB positron emission tomography studies of the serotonin transporter in human brain. *J Cereb Blood Flow Metab*. 2003;23:1096–1112.

(9) Mintun MA, Raichle ME, Kilbourn MR, Wooten GF, Welch MJ. A quantitative model for the in vivo assessment of drug binding sites with positron emission tomography. *Ann Neurol*. 1984;15:217–227.

(10) Paxinos G, Watson C. *The Rat Brain in Stereotaxic Coordinates.* San Diego, CA: Academic Press; 1998:1–286.

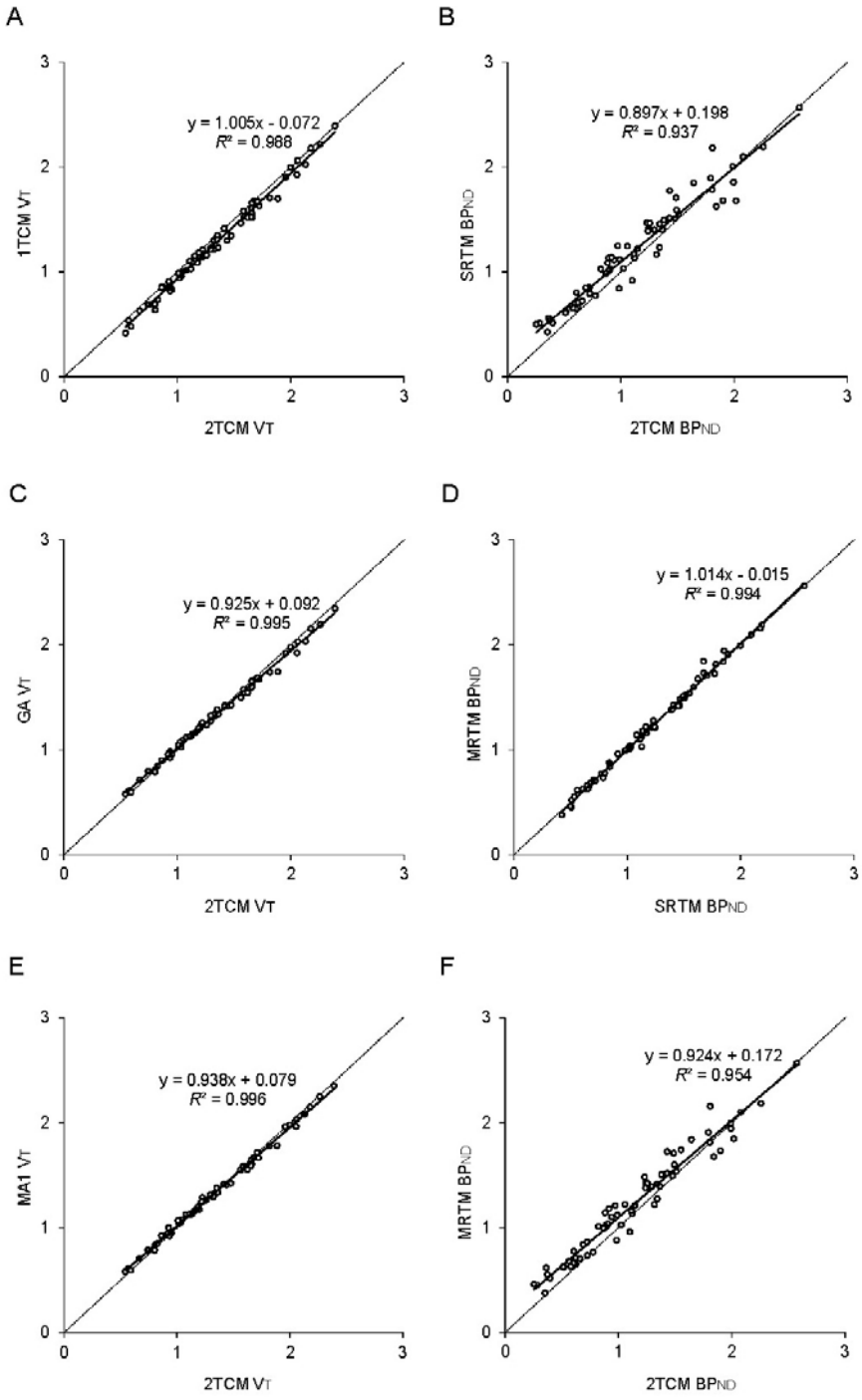

Supplemental Figure 1: Bolus injection experiments: Correlations of the distribution volume (V_T) and binding potential (BP_{ND}) derived by different nonlinear and (multi-) linear methods. (A) Correlation between V_T of the 1- and 2-tissue-compartment model (1/2TCM). (C) Correlation between V_T of the 2TCM and Logan graphical analysis (GA). (E) Correlation between V_T of the 2TCM and multilinear analysis (MA1). (B) Correlation between BP_{ND} derived from the V_T of 2TCM and the simplified reference tissue model (SRTM). (D) Correlation between BP_{ND} based on SRTM and multilinear reference tissue model (MRTM). (F) Correlation between BP_{ND} derived from the V_T of 2TCM and the MRTM. Solid line represents linear regression analysis and dotted line identity. Results of regression are depicted of 13 regions in 5 animals.

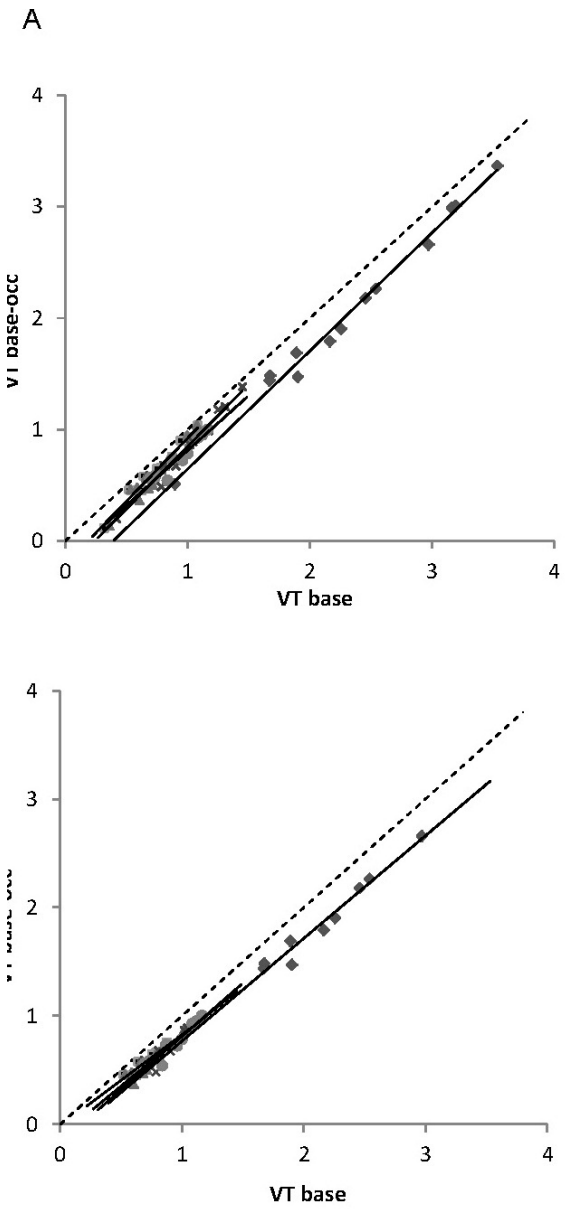

Supplemental Figure 2: Lassen plots (occupancy plots) of the displacement studies. Part A shows the plots including all regions of interest whereas in part B the olfactory bulb and the internally located high-binding regions (caudate-putamen, thalamus, and hippocampus) were excluded.